Whangārei Inner Harbour Flood Modelling

Prepared for:

Northland REGIONAL COUNCIL

eCoast
eTakutai

MOHIO - AUAHA - TAUTOKO
UNDERSTAND - INNOVATE - SUSTAIN

PO Box 151, Raglan 3225, New Zealand
Ph: +64 7 825 0087 I info@ecoast.co.nz I www.ecoast.co.nz

Whangārei Inner Harbour Flood Modelling

Report Status

Version	Date	Status	Approved by
V.1	28 May 2021	Draft	SDG
V.2	25 June 2021	Final	SDG

It is the responsibility of the reader to verify the version number of this report.

Authors

Dougal Greer *BSc (Hons), MSc (Hons)*
Rhys McIntosh *BSc, MSc (Hons)*
Jose Borrero *BSc, MSc, PhD*
Sam O'Neill *BSc, MSc (Hons)*
Jai Davies-Campbell *BSc, MSc (Hons)*

Executive Summary

eCoast Marine Consulting and Research was commissioned by Northland Regional Council to carry out a series of hydrodynamic flood simulations for the upper Whangārei Harbour in Northland, New Zealand. This modelling was undertaken covering the entire harbour with particular focus on the upper harbour region.

This assessment utilises Mean High Water Spring (MHWS) and extreme sea levels derived by Eager and Stephens (2020) to model extreme water level scenarios that correspond to:

- CFHZ0 - 1% Annual Exceedance Probability (AEP) for 2020 water levels
- CFHZ1 - 2% AEP for 2080 water levels
- CFHZ2 - 1% AEP for 2130 water levels
- CFHZ3 – 1% AEP for 2130 water levels under highest sea level rise scenario
- MHWS-10
- MHWS 2080
- MHWS 2130

The modelled processes include open ocean sea level, river flow and wind. The model topography was derived from high resolution LiDAR topography data on land. Overland roughness parameterisation was specific to land cover type and background river flow was derived from river gauge data. All model simulations were undertaken using the HEC-RAS version 6.0.0 modelling suite (Hydraulic Engineering Centre – River Analysis System) developed by the U.S. Army Corps of Engineers. The model was calibrated against river stage at two locations.

Model results were processed into raster files of maximum water surface elevation, maximum water velocity and maximum depth, as well as flood extent shape files for the Council's databases.

Contents

Figures

Tables

1 Introduction

eCoast Marine Consulting and Research was contracted by Northland Regional Council (NRC) to develop a hydrodynamic coastal hazard flood model for the Upper Whangārei Harbour, Northland, New Zealand (Figure 1.1) taking in the rivers of six subcatchments (Figure 1.2). Whangārei Harbour has been divided into multiple 'cells' for the purposes of analysing coastal hazard risk (Figure 1.3) and this study focuses on the cell in the head of the harbour (Figure 1.4).

The objective of this study was to develop a combined hydrodynamic and terrestrial flood model to include the Whangārei harbour in its entirety and tidal areas of the inflowing rivers and its surrounding land. The model used a variable resolution grid with topography interpolated from a 1 m x 1 m 2019 LiDAR dataset. Seven flood scenarios were modelled:

- 1% Annual Exceedance Probability (AEP) 2020 static water level;
- the 2% AEP 2080 static water level,
- the 1% AEP 2130 static water level,
- the 1% AEP 2130 static water level under highest sea level rise scenario
- the 10% exceedance mean high water spring (MHWS) level,
- the 2080 MHWS level, and,
- the 2130 MHWS level.

It is expected that these results will help inform NRC of the areas that will require stopbank upgrades or other flood aversion procedures, as well as planning for the impacts of SLR (sea level rise).

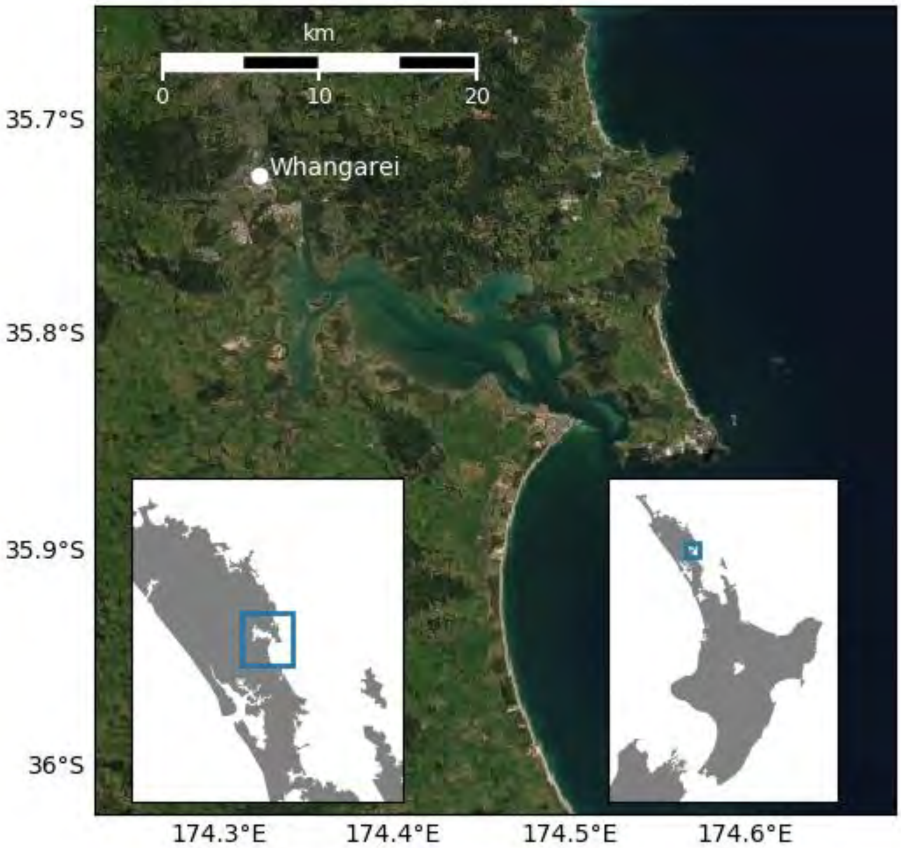

Figure 1.1: Whangārei Harbour located on the northeast coast of Northland.

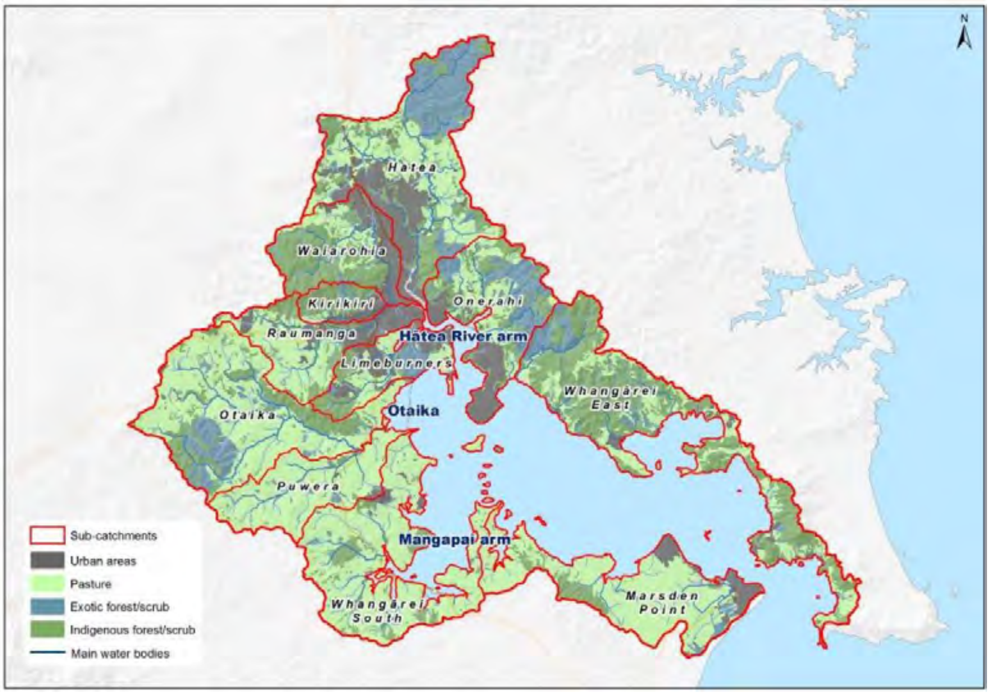

Figure 1.2: Subcatchments of the Whangārei Harbour, image from NRC and Whangārei District Council (2012). Flows from the Onerahi, Hātea, Waiarohia, Kirikiri, Raumanga and Limeburners subcatchments were included in the flood modelling.

Figure 1.3: Whangārei Harbour delineated into coastal cells for the purposes of coastal flood hazard. Note that the coastal flood hazard results are from a separate study (source: NRC).

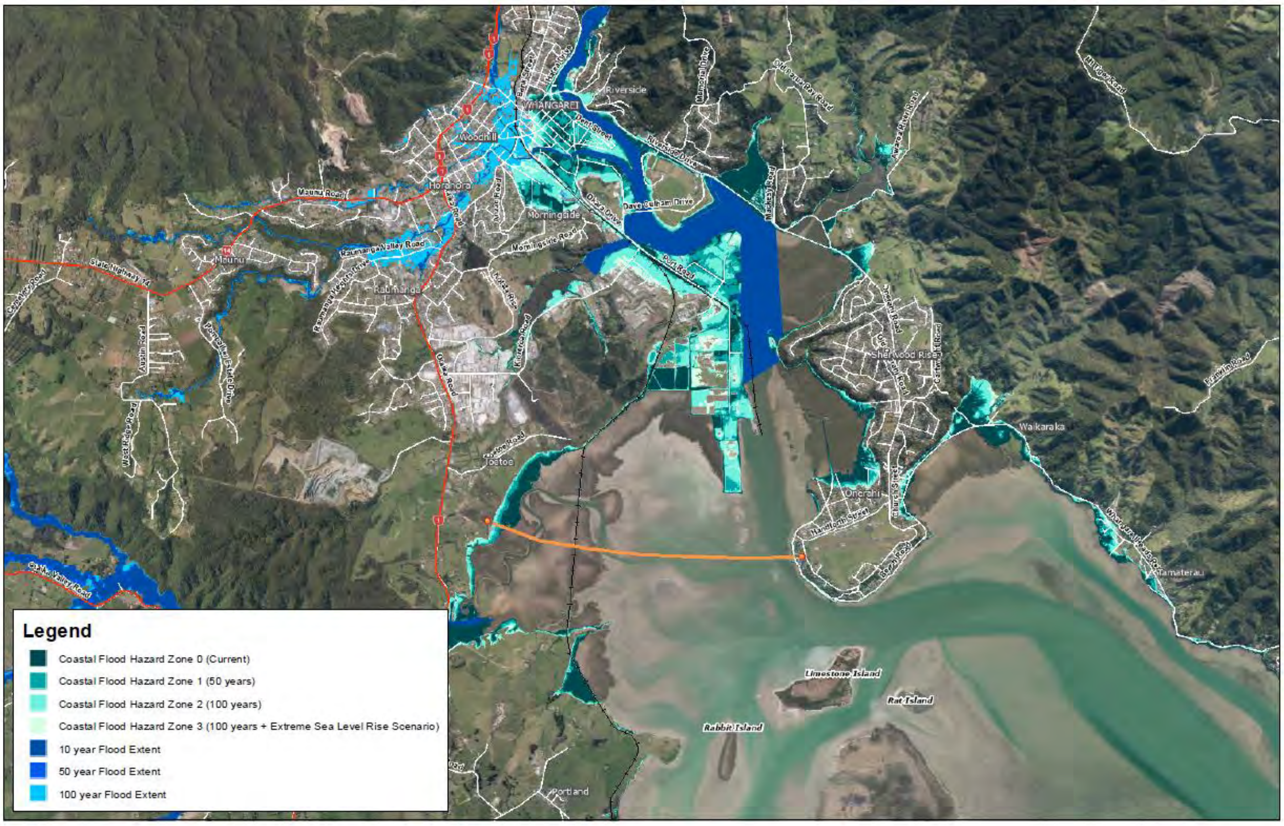

Figure 1.4: Coastal hazard cell in the head of Whangārei Harbour that is the focus of this study. Note that the coastal flood hazard results are from a separate study (source: NRC).

1.1 Project Scope and Methodology

The following methodology has been applied to this project:

a) Collate Whangārei Harbour bathymetry and merge with 2019 LiDAR.
b) Set up flood model domain.
c) Use flexible mesh from 50 m x 50 m to 15 m x 15 m to 1 m x 1 m, with 1 m x 1 m resolution used where required to enable identification of features such as roads/stopbanks potentially blocking flow.
d) Where necessary fill unexpected gaps in stopbanks in DTM.
e) Define roughness based on assumed terrain and best-practice guidelines.
f) Calibrate model against measures sea level/river stage data.
g) Derive scenario boundary conditions based on previous studies (Eager and Stephens, 2020) and measured data records.
h) Recorded tidal signal adjusted to MHWS10 (10% exceedance), MHWS 2080, MHWS 2130, CFHZ0, CFHZ1, CFHZ2 and CFHZ3 elevations.
i) Sensitivity test for roughness and other model parameters/boundaries.
j) Run seven inundation scenarios and output shapefiles for flow elevation, depth, velocity for each and supply to Council for review.
k) Test model levels against bathtub flood modelling held by NRC[1].
l) Concise report summarising methodology, model set up, assumptions made, sensitivity testing details and results for Council review.
m) Make any changes required based on Council review (provisional Item).

1.2 Datums and Coordinates

All elevations (levels) presented in this report are presented in terms of New Zealand Vertical Datum (NZVD) 2016. The coordinate reference system used for this project is New Zealand Transverse Mercator 2000 (NZTM2000). Note that the extreme sea levels from Eager and Stephens (2020) are referenced to OTP-64. A conversion of 0.099 m was applied to convert them to NZVD[2].

[1] https://nrcgis.maps.arcgis.com/apps/webappviewer/index.html?id=81b958563a2c40ec89f2f60efc99b13b

[2] https://www.geodesy.linz.govt.nz/concord/

2 Model Set Up

The modelling methodology presented here focuses on the flood risk due to elevated sea level, though wind and river flow are also included. The model takes in Whangārei Harbour in its entirety and transforms the open ocean sea level through the harbour and up the Hātea river and other smaller streams.

2.1 Model Description

The hydrodynamic modelling was undertaken using the HEC-RAS 6.0.0 modelling suite (Hydraulic Engineering Centre – River Analysis System, 2016) developed by the U.S. Army Corps of Engineers as part of the "Next Generation" of hydraulic engineering software. In addition to the river analysis system, the model encompasses rainfall-runoff analysis (HEC-HMS), reservoir system simulation (HEC-ResSim), flood damage analysis (HEC-FDA and HEC-FIA) and real-time river forecasting for reservoir operations (CWMS).

HEC-RAS is capable of simulating two-dimensional unsteady flow through a full network of open channels, alluvial fans and floodplains and can perform subcritical, supercritical and mixed flow regime calculations. The basic computational procedure solves the full-dynamic two-dimensional Saint Venant equations (2D shallow water equations) using an implicit finite difference method. Further detail about the model can be found in the HEC-RAS 6.0 User's Manual.

2.2 Preparation of Digital Terrain Model and Model Grid

The Whangārei Harbour Digital Terrain Model (DTM), shown in Figure 2.1, was created based on measured topographic and bathymetric data. High resolution 1 m x 1 m LiDAR topography data was supplied by the NRC, while additional low resolution topography data, used exclusively outside of the modelled cell (Figure 1.3), was sourced from the Shuttle Radar Topography Mission (SRTM). Bathymetric data was extracted from hydrographic charts provided by Land and Information New Zealand (LINZ).

Model grids, (known as 2D flow areas in HEC-RAS), were constructed for the Whangārei Harbour model encompassing all open channels, alluvial fans, floodplains and other flood pathways. The initial cell size was set to 50 m x 50 m for the permanently submerged areas of the harbour and 15 m x 15 m for intertidal and land areas. This resulted in a mostly rectilinear mesh, with the exception of the cells adjacent to the grid boundaries that take an irregular shape in order to 'snap' to the shape of the 2D flow area. The grid extents are displayed in Figure 2.1, while an example of a high-resolution area is illustrated in Figure 2.2.

Any feature acting as a barrier to flow identified in each of the model terrains such as stopbanks, raised roads, river and creek banks, canal banks, drainage ditch banks, etc., required break lines to be enforced into the grid. This means that such features received greater cell resolution on each of their sides as well as forcing cell faces along their crest lengths (Figure 2.2). The smallest grid cells created as a result of this procedure were 1 m x 1 m, matching the LiDAR resolution of the underlying terrain.

During the model validation process some artefacts within in the DTM were discovered. The DTM was modified accordingly.

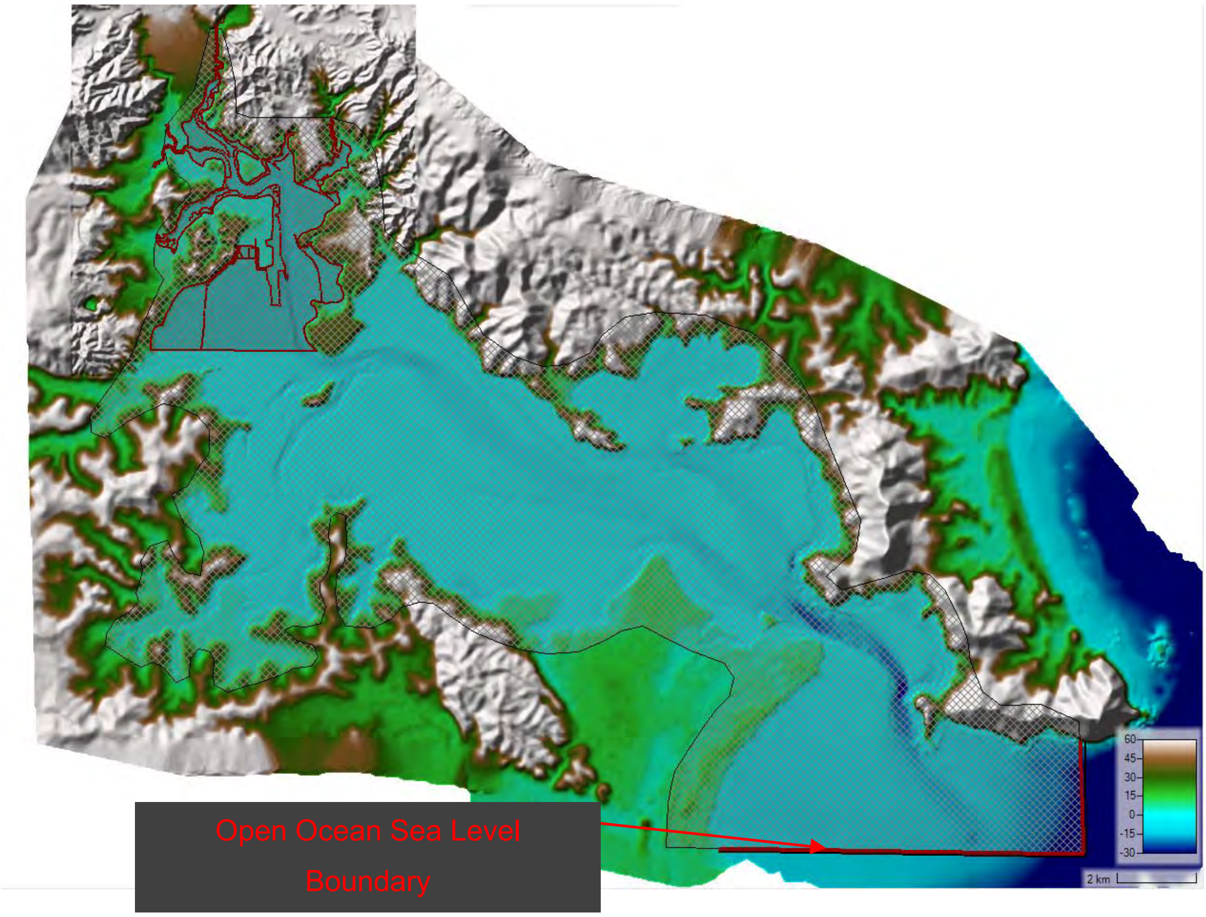

Figure 2.1: Whangārei Harbour DTM, derived from LiDAR, SRTM and hydrographic chart data, with the grid extents overlaid. Note that the colour scale refers to metres relative to NZVD2016. The boundary where storm surge conditions were applied is shown to the south of the harbour.

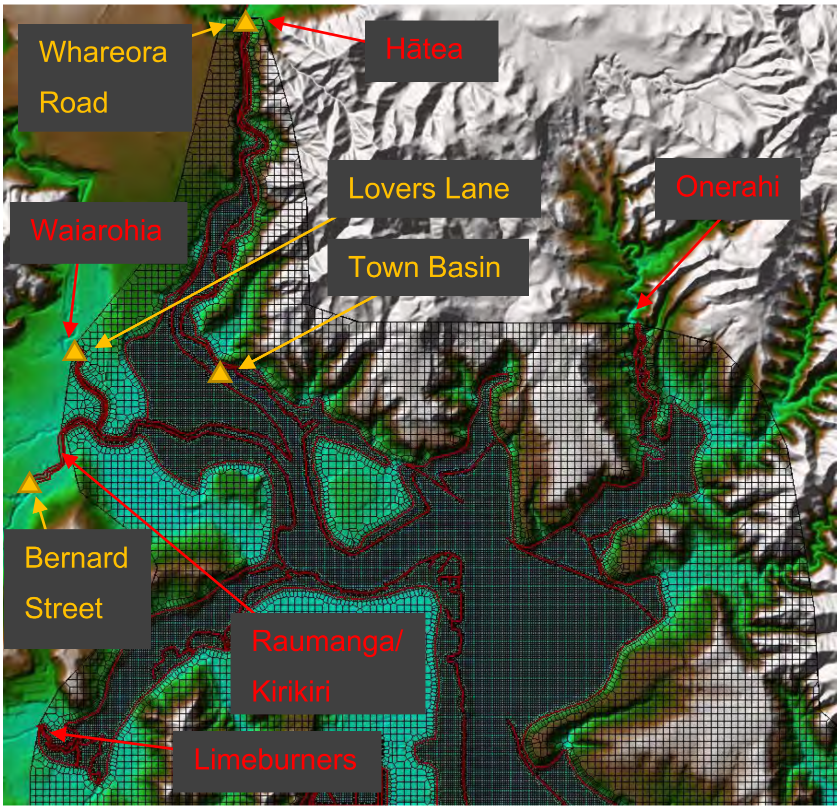

Figure 2.2: Northern section of the Whangārei Harbour model grid and DTM, showing higher cell resolution around refinement areas and break lines. All of the river/stream model boundaries are indicated in red while all of the river/stream flow gauges are shown by orange triangles.

2.3 Roughness

HEC-RAS has the capability of defining spatially variable roughness within the model domain. This allows for realistic representation of the resistance to flood flows over rough land cover such as fernlands or mangroves. This was achieved by assigning Manning's roughness coefficients (Manning's n values) to each land use type recognised in the region. Land use shape files for each of the three model domains were acquired from the Land Resource Information Systems (LRIS) data portal and Manning's n values were assigned following U.S. Geological Survey Water Resources Division (1984) and Chow (1959). Figure 2.3 presents the Manning's n values used along with an example of the spatial distribution of the different land uses. It is also important to note that in regions where a land use was not specified, a default Manning's n value of 0.018 was applied to all model runs. Manning's n values were adjusted to test for sensitivity and to calibrate the model (see Sections 2.6 and 2.7 for more detail).

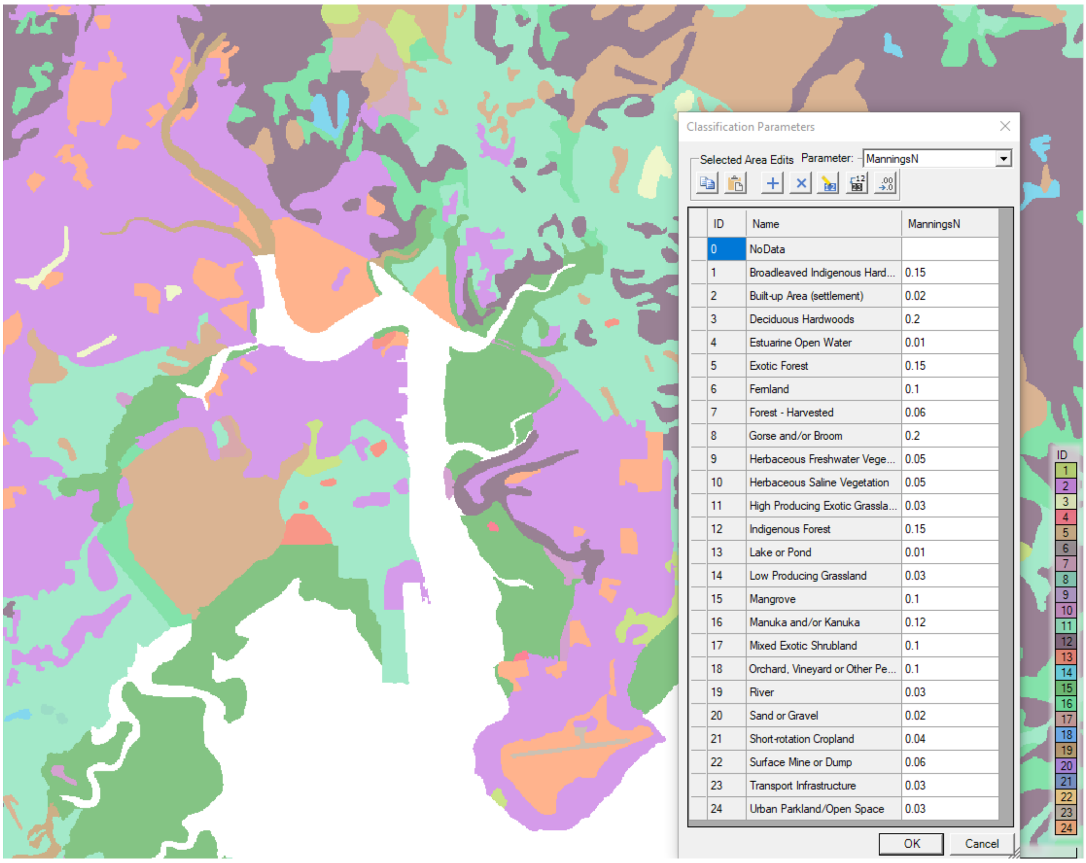

Figure 2.3: Upper Whangārei Harbour model showing Manning's n values for spatially varying roughness.

2.4 Model Scenarios

Coastal Flood Hazard Zone (CFHZ - consisting of storm tide, wave set up and sea-level rise) and Mean High Water Spring (MHWS) levels derived by Eager and Stephens (2020) have been assessed as follows: For each scenario, a tidal time series has been derived with maxima consistent with the maximum water level values in Table 2.1.

CFHZ0, CFHZ1, CFHZ2 and CFHZ3 represent storm surge levels corresponding to the current (2020) 1% Annual Exceedance Probability (AEP), 2% AEP with 2080 sea-level rise (SLR), 1% AEP with 2130 sea-level rise and 1% AEP with highest sea level rise scenario for 2130 respectively. MHWS-10 is the elevation exceeded by the highest 10% of all high tides. Sea level rise values were provided by NRC.

Table 2.1: Water levels at Marsden Point for each modelled scenario in m (NZVD), derived from Tonkin and Taylor (2020). The maximum water level is the sum of the storm surge/MHWS level and sea level rise (SLR).

Scenario Name	Storm Surge	MHWS-10 Amplitude	SLR	Max. Water Level
CFHZ0 (1% AEP)	1.70	-	0	1.70
CFHZ1 (2% AEP)	1.63	-	0.60	2.23
CFHZ2 (1% AEP)	1.70	-	1.20	2.90
CFHZ3 (1% AEP)	1.70	-	1.50	3.20
MHWS-10	-	1.05	0	1.05
MHWS 2080	-	1.05	0.60	1.65
MHWS 2130	-	1.05	1.20	2.25

2.5 Boundary Conditions

Open ocean sea level boundary conditions for the model runs were created by extracting a tidal curve from the long-term sea level record at the Marsden Point tide gauge associated with the largest sea level in the record (see Figure 2.4). A full tidal cycle previous to the extreme sea level was also included in the record for model spin up. For each scenario, an offset was applied to the sea level record so that the maximum sea level (the second high tide peak) matched the maximum water level values in Table 2.1. Note that the sea levels from Eager and Stephens (2020) are referenced to OTP-64 and an offset of -0.099 m was applied to the sea level boundary conditions to change the reference vertical datum to NZVD. All sea level boundary condition time series are presented in Appendix B.

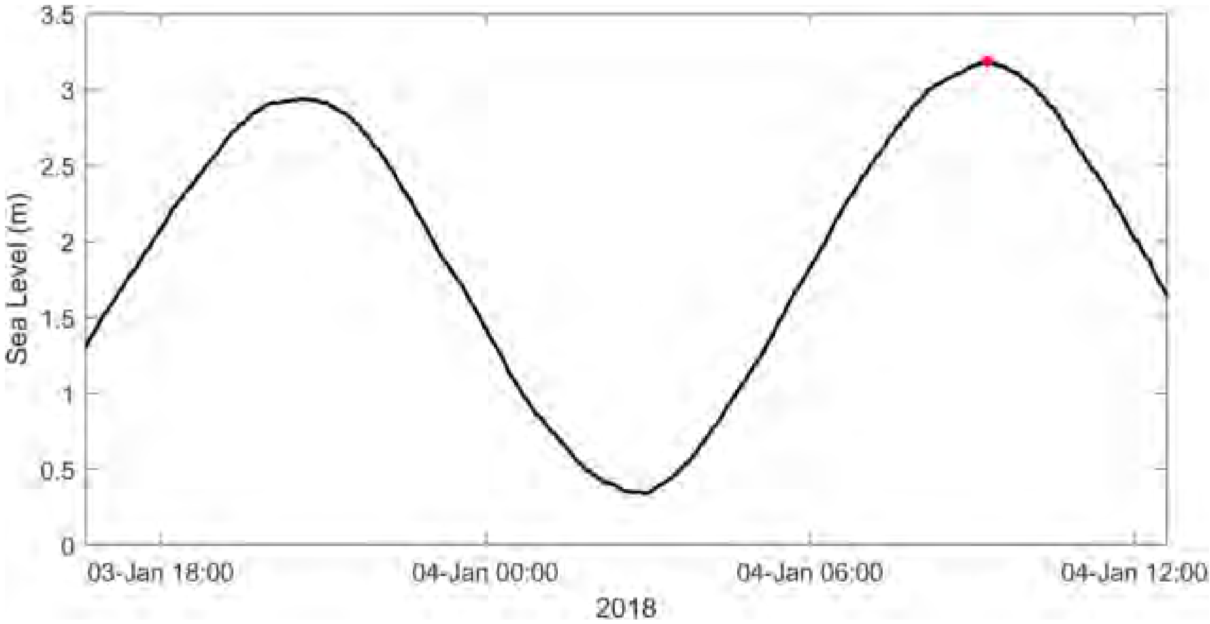

Figure 2.4: Open ocean sea leave boundary condition used for the flood modelling (referenced to LAT). The timeseries was offset by an appropriate to generate specific maximum sea levels for each scenario. The red dot on the second high tide indicated the largest sea level in the record.

The extreme sea levels on the open coast incorporate all non-tidal effects including wind setup. However, within the Whangārei harbour additional wind setup is expected to occur over the shallow estuary. Metocean conditions that lead to elevated sea level are likely to be associated with increased wind speed (e.g. low atmospheric pressure). Analysis was undertaken of wind records coincident with the tide gauge records. Sea level anomaly (i.e. non-tidal sea level variability) was filtered from the Marsden point tide gauge record from 31-Jul-1999 to 30-Dec-2019 using harmonic tidal analysis (Codiga, 2011). As in the Eager and Stephens (2020) analysis, the anomaly was extracted as skew surge (Batstone et al., 2013) which is the largest difference between the predicted tide and the measured sea level over each tidal cycle. Hourly recorded wind data was sourced from the Whangārei Aero AWS[3] spanning the dates of 02-Jun-1998 and 01-Jan-2013. Wind records were compared with coincident skew surge values to investigate any correlation between the signals. For this analysis, the wind records were restricted to those where wind direction is from between 90 and 120 degrees i.e. along the length of the harbour leading from the mouth the head of the harbour. The results of regression analysis comparing wind speed with skew surge are shown in Figure 2.5. This analysis shows a reasonably weak positive relationship (r^2 = 0.32) between the wind speed and skew surge. The results of this analysis were used to provide wind speeds associated with annual exceedances. These wind speeds (with an associated wind direction of 105°) were applied in the model scenarios with 1% and 2% annual exceedance probabilities. For the MHWS scenarios, wind was not applied in the model.

[3] https://cliflo.niwa.co.nz/

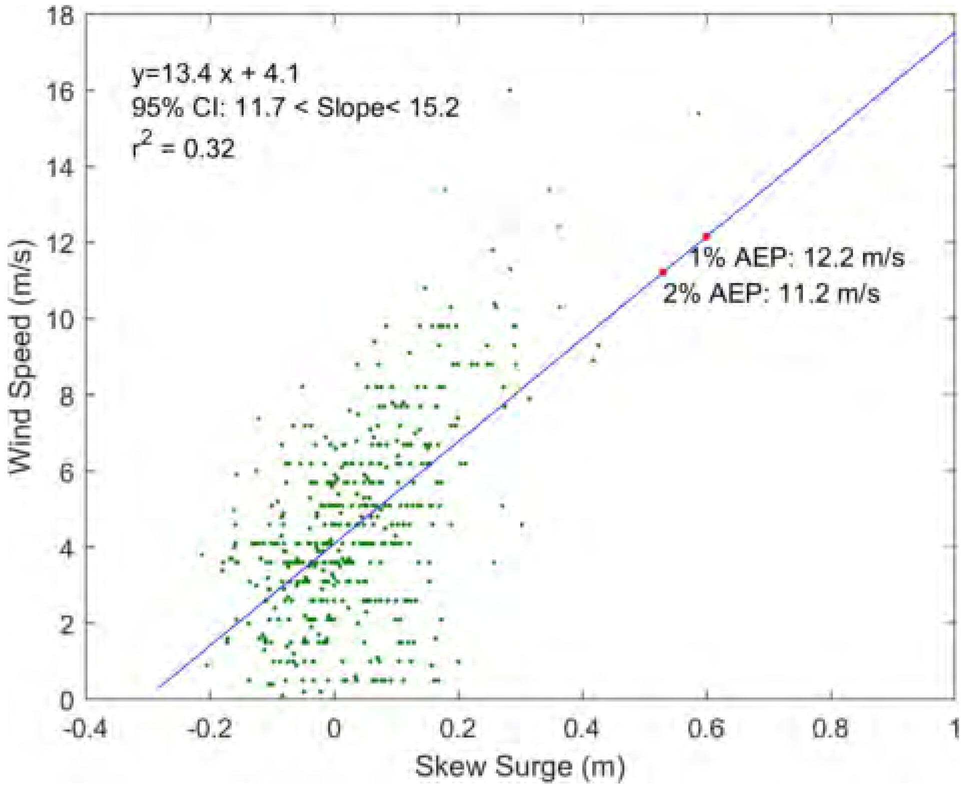

Figure 2.5: Regression analysis relating skew surge to wind speed aligned with the main channel of the Whangārei Harbour.

As per the project scope, a constant median flow rate was applied to inflowing rivers and streams (see Figure 1.2 for the subcatchments of the Whangārei Harbour). Only three of the six rivers/streams included in the model had flow gauge data available, specifically the Hātea River, Raumanga Stream and Waiarohia Stream. The median flows calculated for the Hātea at Whareora Road, Raumanga at Bernard Street and Waiarohia at Lovers Lane flow gauges (Figure 2.2) were 0.581 m^3/s, 0.204 m^3/s and 0.127 m^3/s respectively. Analysing the terrain of these subcatchments, the proportion of the subcatchments upstream and downstream of the flow gauge was determined, and the median flows applied to the model were scaled up to represent the subcatchments in their entirety (Table 2.2). The remaining modelled streams, the Onerahi, Limeburners and Kirikiri, were attributed flow rates by applying a multiplier to the median flow of the nearest known subcatchment based on the proportional areas of the subcatchments. The nearest gauged subcatchments to the Onerahi, Limeburners and Kirikiri subcatchments are the Hātea, Raumanga and Raumanga respectively. Because the Raumanga Stream flow gauge was only approximately 300 m upstream of its confluence with the Kirikiri Stream, the flows for both subcatchment were combined before being applied to the model downstream of the confluence (see Figure 2.2 for river boundary locations).

Table 2.2: Modelled subcatchments of the Whangārei Harbour and their corresponding area and median river flows. Bold flow values indicate the final flow value used in the model. Note that the Raumanga and Kirikiri stream flows were combined in the model.

Subcatchment	Grouped with	Area (km²)	Group area (km²)	Upstream area (km²)	Multiplier	Median gauge flow (m³/s)	Median subcatchment flow (m³/s)	Median flow grouped (m³/s)
Hātea	-	44.7	-	40.6	1.09	0.581	**0.634**	
Waiarohia	-	18.9	-	18.7	1.01	0.127	**0.128**	
Onerahi	-	24.1	-	-	-	-	**0.342**	
Limeburners	-	12.8	-	-	-	-	**0.166**	
Kirikiri	Raumanga	5.6	22.9	-	-	-	0.073	**0.297**
Raumanga	Kirikiri	17.3	-	15.6	1.10	0.204	0.224	-

2.6 Model Calibration and Validation

The modelled water levels were calibrated to the recorded water levels at the Hātea at Town Basin stage gauge (Figure 2.2), which is influenced by both tides and river flows. The model was simulated for an eight-day period from 20/01/2011 – 28/01/2011, which included periods of lower and higher river flows. The roughness of the model bathymetry, which was found to be relatively sensitive to changes, was adjusted until the appropriate water levels were achieved (Figure 2.6). The modelled water levels generally agreed with the measured levels, especially during high tides, which is appropriate for storm surge modelling.

To validate the model, the MHWS-10 scenario (Table 2.1) was used to make sure there were no stopbank breaches in the model domain, which would not be expected under mean high water spring conditions. As mentioned in Section 2.2, breaches were seen in some areas due to artefacts in the DTM, which were then filled manually in an iterative process. In the end a satisfactory MHWS-10 validation was achieved and is shown in Appendix A.

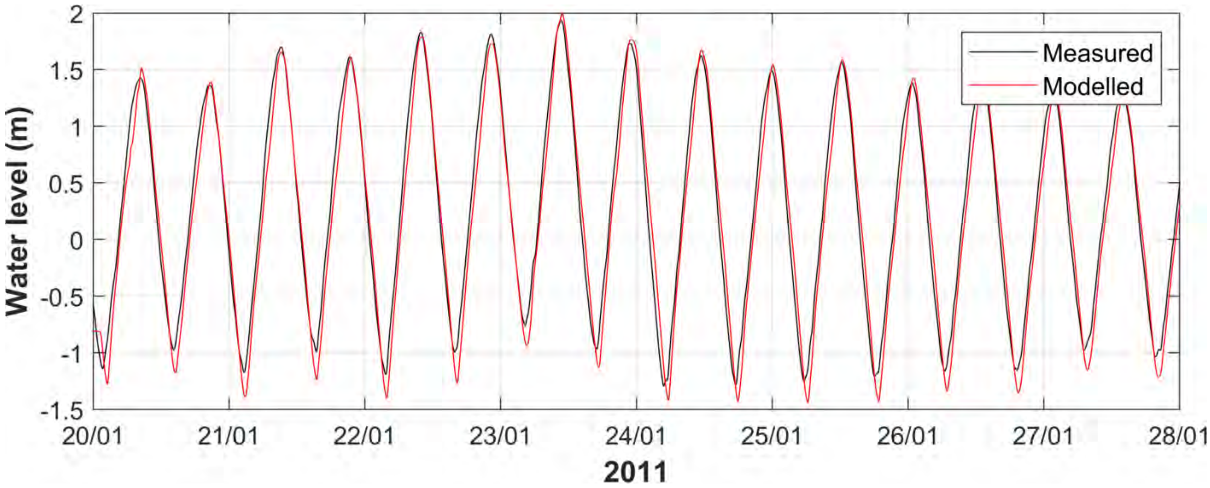

Figure 2.6: Measured and modelled water levels at the Hātea at Town Basin stage gauge from 20-Jan-2011 to 28-Jan-2011.

2.7 Sensitivity Analysis

Model sensitivity was tested on three parameters: model overland roughness/friction, wind conditions and river flows. These parameters were tested by adjusting the CFZ0 simulation and then comparing the flood extents with the original simulation. Table 2.3 shows this comparison in terms of absolute flooding extent areas and flood extent area change compared to the original CFHZ0 scenario.

Table 2.3: CFHZ0 sensitivity analysis comparing the flood extents of three scenarios with either adjusted friction, wind parameters or river flow to the original CFHZ0 simulation.

Scenario	Flooding extent area (km^2)	Area change compared to original (km^2)
Original	136.88	-
10% friction reduction	136.89	0.003
No wind	136.59	-0.296
100-year river flows	136.89	0.011

2.7.1 Overland Roughness

To test the sensitivity of the model to reductions in overland roughness, all on-land Manning's n values (Figure 2.3) were reduced by 10%. This reduction in overland roughness was found to increase flood extents by a negligible amount, which contrasts with the bathymetric roughness coefficients which were found to be a sensitive parameter during model calibration (Section 2.6).

2.7.2 Wind

To test how much the inclusion of wind in the model simulations affected the flood extents, the CFHZ0 scenario was simulated with no wind inputs. The inclusion of wind was found to be important in some sections of the upper Whangārei Harbour, while in others it had no effect (Figure 2.7). Most notably, the wind had a large effect on the Raumanga/Waiarohia Stream, which is orientated at a similar angle to the wind (105° from north). This test indicates that both wind speed and direction will affect the extents and locations of flooding.

Figure 2.7: CFHZ0 flood extents in the upper Whangārei Harbour with 1% AEP wind conditions (red) and no wind (blue).

2.7.3 River Flows

As with wind conditions, it is likely that elevated sea levels will be associated with increased river flow, so additional analysis was undertaken to investigate the sensitivity of model results to increased river flow associated with extreme sea levels. River flow data was sourced from the Hātea at Whareora Road river flow gauge from 17-Sep-2007 to 10-Aug-2015. The flow data has a sampling rate of 15 minutes, so the record was decimated to an hourly sampling interval to align with the tide record. A weak correlation (r^2 = 0.1) between the two signals was established and used to provide flow rates associated with the 1% and 2% AEP sea level conditions. These flow rates were scaled up to represent the entire Hātea subcatchment and then applied to the other modelled streams using proportional subcatchment area to the Hātea subcatchment to scale down the flows (see Table 2.2 for subcatchment data).

The CFHZ0 scenario with 1% AEP river flows was simulated and found to only have a very localised effect on flooding extents. Figure 2.9 shows an example of this effect on the upper Hātea River, where local flooding increased under 1% AEP river flows. Some 500 m downstream, however, the increased river flow can be seen to have no effect on the flood extents further downstream. This was the same downstream from all of the river inputs. This indicates that there would need to be a much larger flow event to have any effect on areas such as the Whangārei CBD.

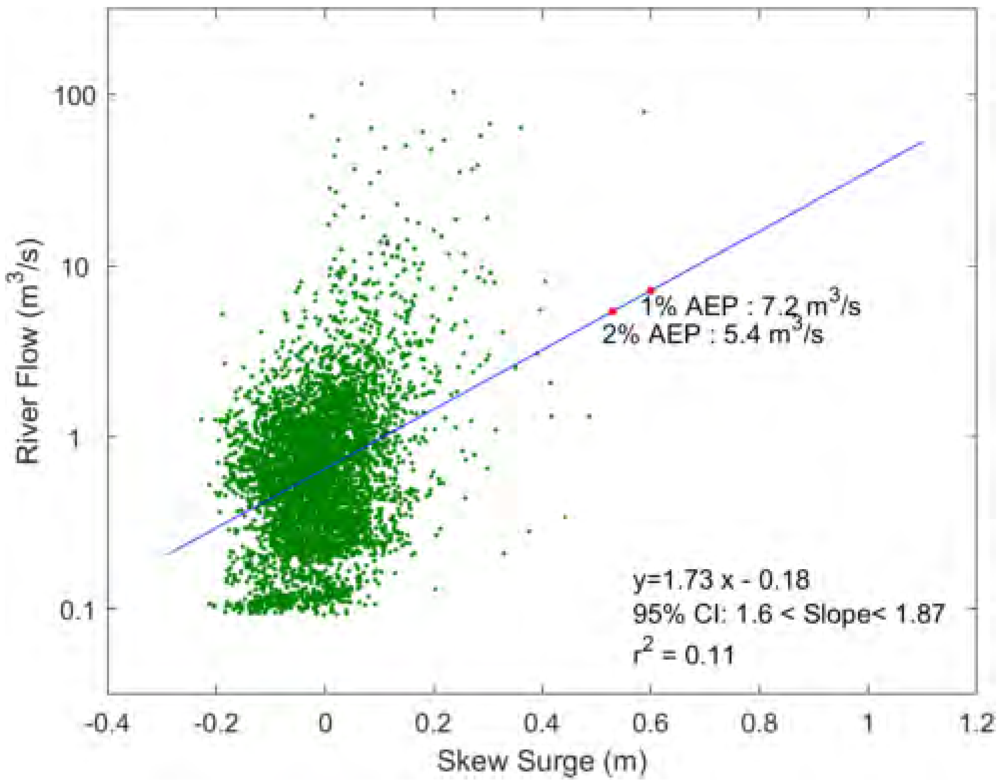

Figure 2.8: Regression analysis relating skew surge to river flow in the Hātea River.

Figure 2.9: CFHZ0 flood extents in the upper Hātea River with median river flows (red) and 1% AEP river flows (blue). Note that at a given point downstream the increased river flow ceases to affect the flood extents.

3 Results

Model results from the seven inundation scenarios presented in Table 2.1 were processed into raster files of maximum water surface elevation, maximum water velocity and maximum depth, as well as flood extent shape files. All model results are displayed in Appendix A. As per the project scope, results were postprocessed to remove flooded model grid cells with a maximum depth of less than 100 mm and ponding areas of less than 2000 m^2.

The Coastal Flood Hazard Zone (CFHZ) scenarios were compared with the NRC bathtub modelling results held by NRC (Figures Figure 3.1 through Figure 3.4). The flooding extents were mostly similar, with the exception of small areas where the bathtub model predicted greater flooding. One of these areas is the suburb of Morningside, Whangārei, which is just south of Raumanga Stream. Flood extents for CFHZ0, CFHZ1 and CFHZ2 (Figure 3.1, Figure 3.2 and Figure 3.3 respectively) were notably greater in the bathtub model in this area, while the CFHZ3 flood extents in the area were similar for both models (Figure 3.4).

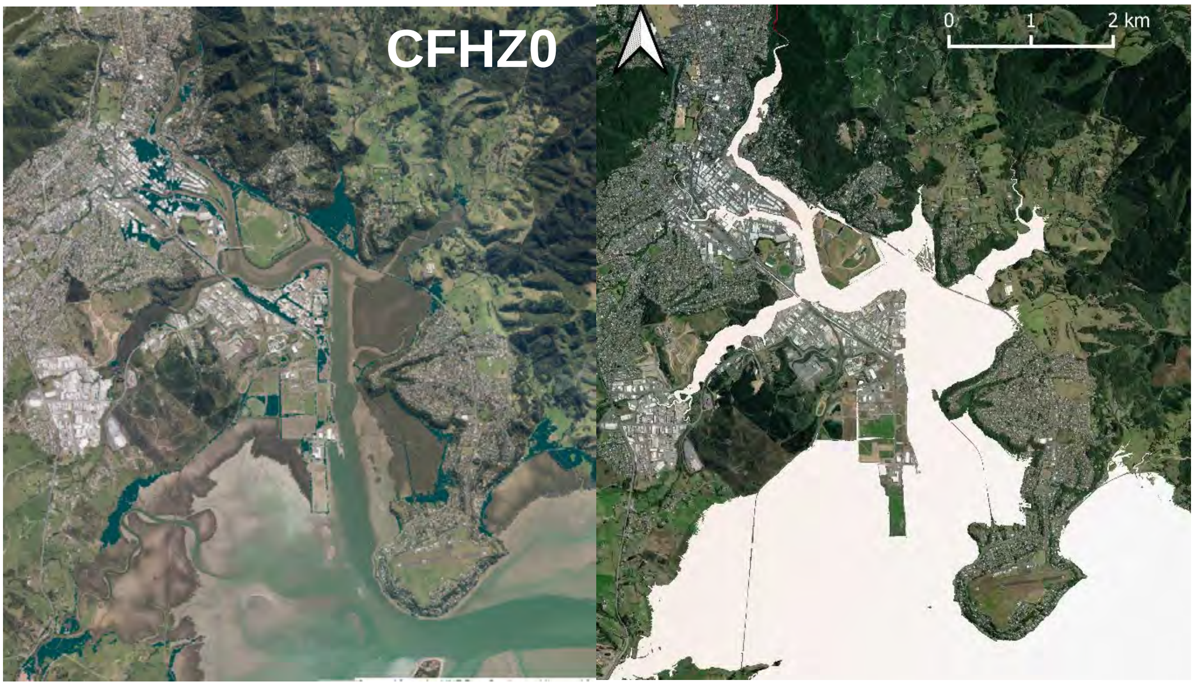

Figure 3.1: Comparison of NRC bathtub modelled flood extents (left) with the HEC-RAS modelled flood extents (right) for CFHZ0.

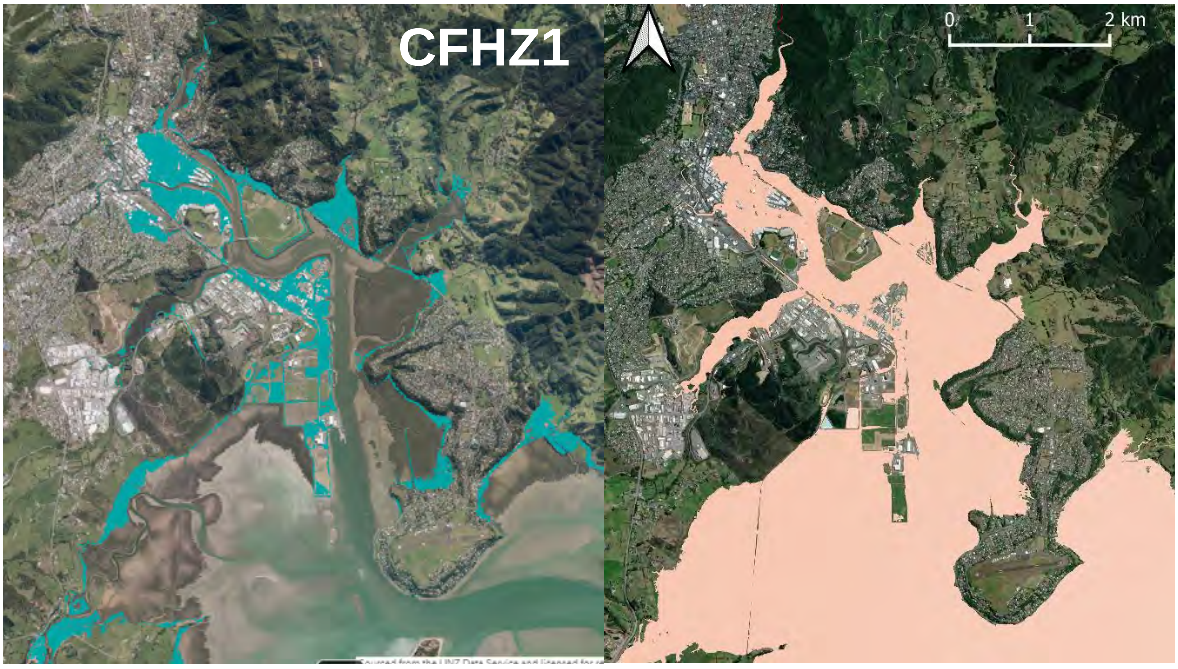

Figure 3.2: Comparison of NRC bathtub modelled flood extents (left) with the HEC-RAS modelled flood extents (right) for CFHZ1.

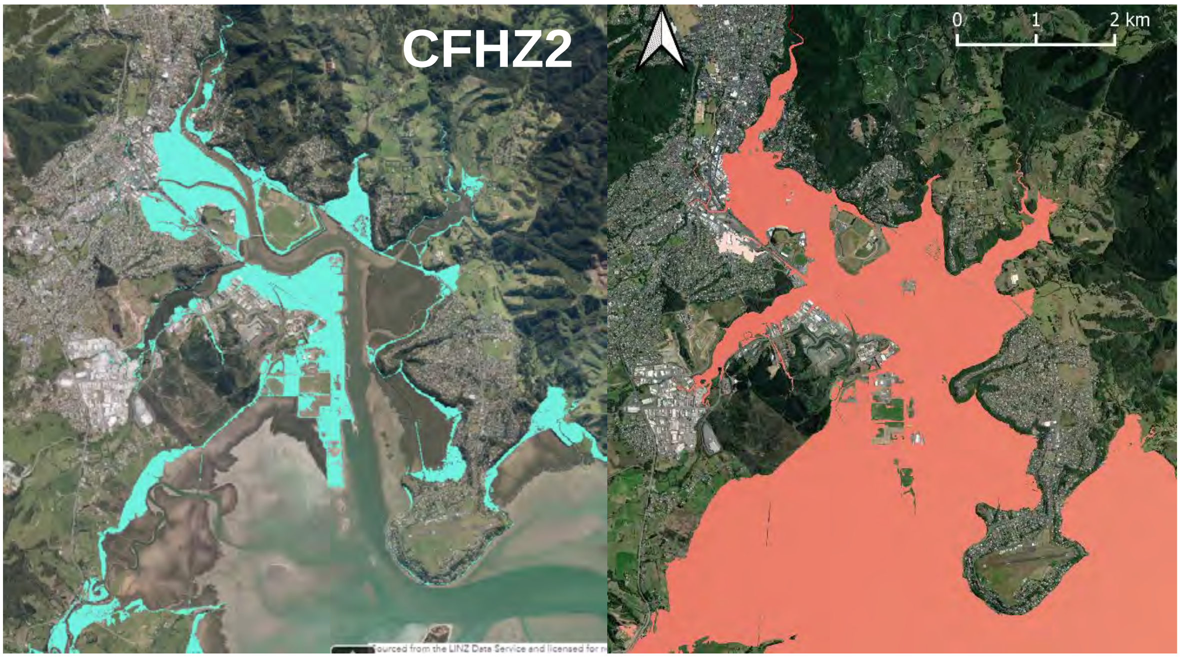

Figure 3.3: Comparison of NRC bathtub modelled flood extents (left) with the HEC-RAS modelled flood extents (right) for CFHZ2.

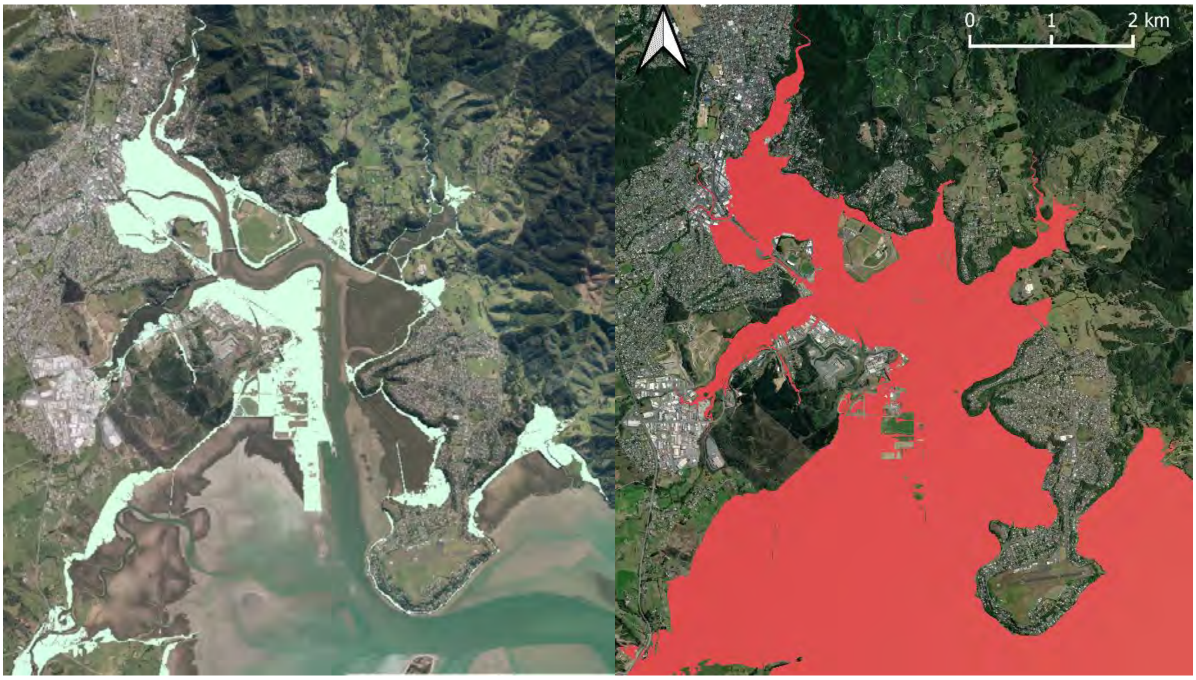

Figure 3.4: Comparison of NRC bathtub modelled flood extents (left) with the HEC-RAS modelled flood extents (right) for CFHZ3.

4 Study Limitations and Assumptions

1) Drainage structures were not represented in the HEC-RAS model domains. These features can alter the flow of floodwaters both onto and away from low-lying regions.
2) Some fine-scale stopbank structures are not well resolved by the LiDAR data. Sometimes these structures are manually surveyed, but in this region no such surveys were available. Consequently, fine-scale stopbanks may not be represented comprehensively in the model.

5 Summary and Conclusions

1) A hydrodynamic model (HEC-RAS version 6.0.0) of the upper Whangārei Harbour was created to simulate inland flooding under seven extreme scenarios:
   - 1% Annual Exceedance Probability (AEP) 2020 static water level;
   - the 2% AEP 2080 static water level,
   - the 1% AEP 2130 static water level,
   - the 1% AEP 2130 static water level under highest sea level rise scenario,
   - the 10% exceedance mean high water spring (MHWS) level,
   - the 2080 MHWS level, and,
   - the 2130 MHWS level.
2) The model was sensitivity tested for domain size, cell size and overland roughness. wind conditions and river flow.
3) The model was calibrated by using measured sea level and river stage data and adjusting model parameters to obtain an adequate reproduction of measured values.
4) Model results were compared with bathtub flood modelling held by NRC and found to be generally similar with the bathtub modelling predicting greater flooding in some areas.
5) Maximum water surface elevation, maximum water velocity and maximum depth shape files of coastal flood extents have been supplied to NRC.

References

Batstone, C., Lawless, M., Tawn, J., Horsburgh, K., Blackman, D., McMillan, A., Worth, D., Laeger, S., Hunt, T., (2013) A UK best-practice approach for extreme sea-level analysis along complex topographic coastlines. Ocean Engineering, 71: 28-39. http://dx.doi.org/10.1016/j.oceaneng.2013.02.003

Codiga, D. L. (2011). Unified tidal analysis and prediction using the UTide Matlab functions.

Chow, V.T., (1959). Open-Channel Hydraulics: New York, McGraw-Hill, 680 p.

Eager, C. and Stephens, S., (2020). Northland Sea Level Analysis, Memo, prepared for Northland Regional Council.

HEC-RAS (2016). U.S. Army Corps of Engineers Institute for Water Resources Hydraulic Engineering Centre River Analysis System – User's Manual Version 5.0.

Northland Regional Council and Whangārei District Council (2012). Whangārei Harbour Water Quality Improvement Strategy.

U.S. Geological Survey Water Resources Division (1984). Guide for Selecting Manning's Roughness Coefficients for Natural Channels and Floodplains. Technical Report number FHWA-TS-84-204.

Appendix A. Model Result Maps

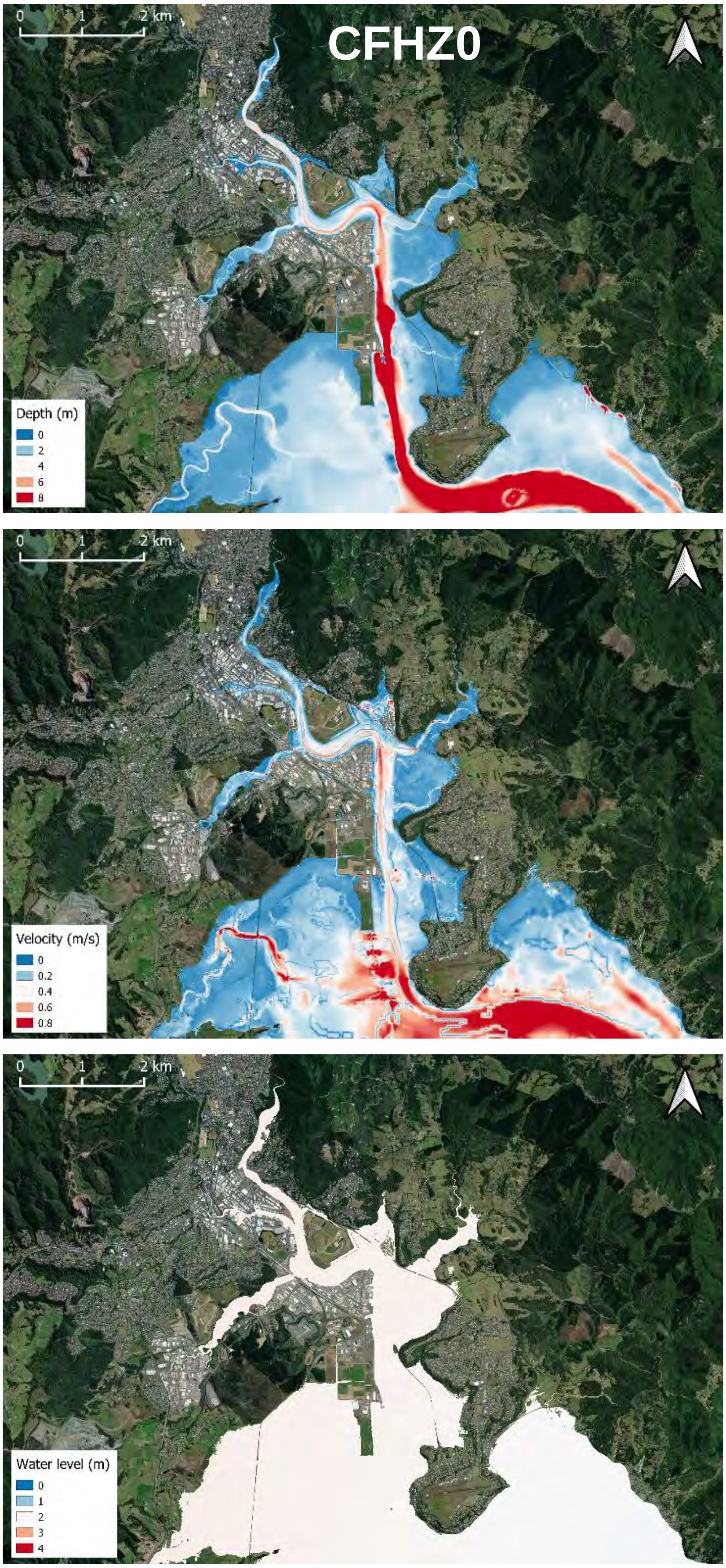

Figure A.1: Modelled maximum depth (upper), velocity (middle) and water level (lower) for the CFHZ0 scenario.

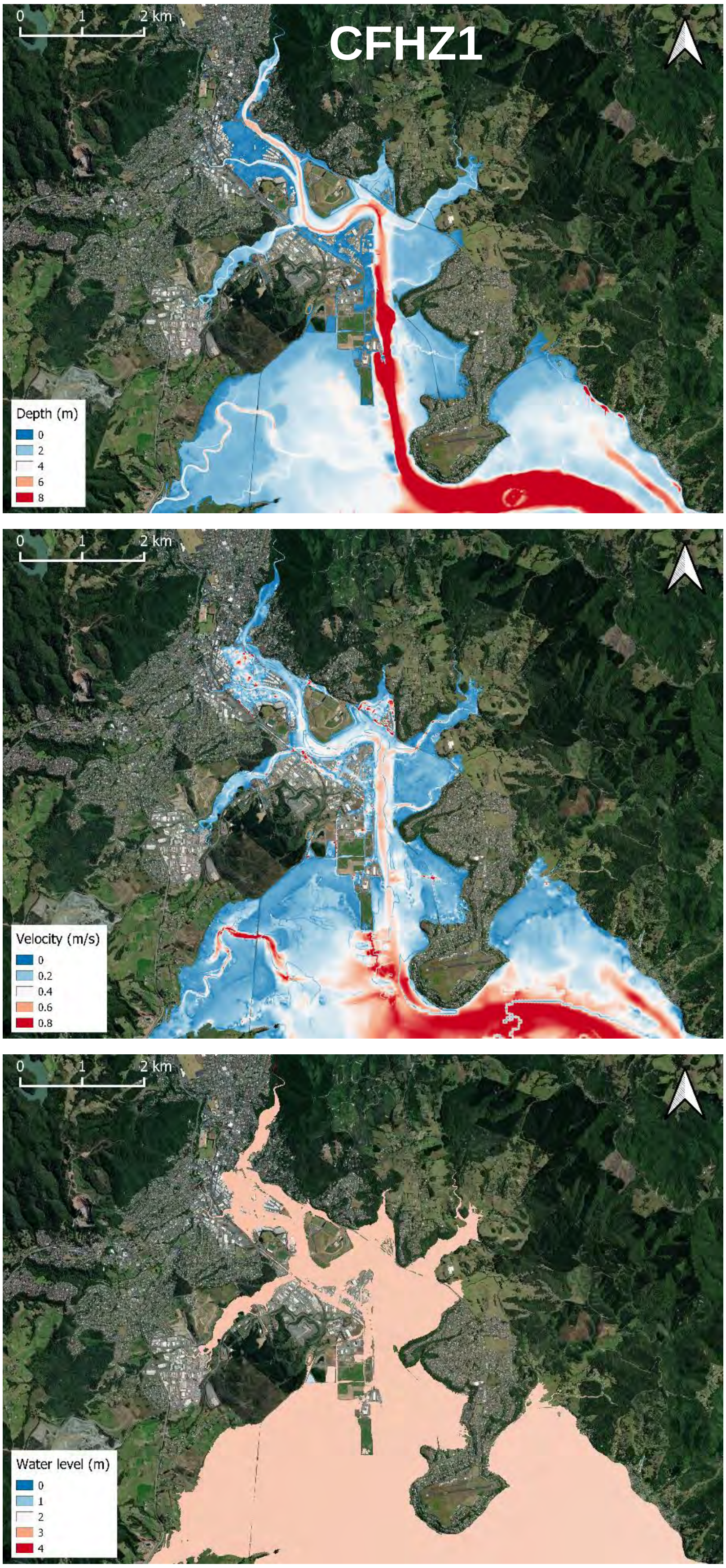

Figure A.2: Modelled maximum depth (upper), velocity (middle) and water level (lower) for the CFHZ1 scenario.

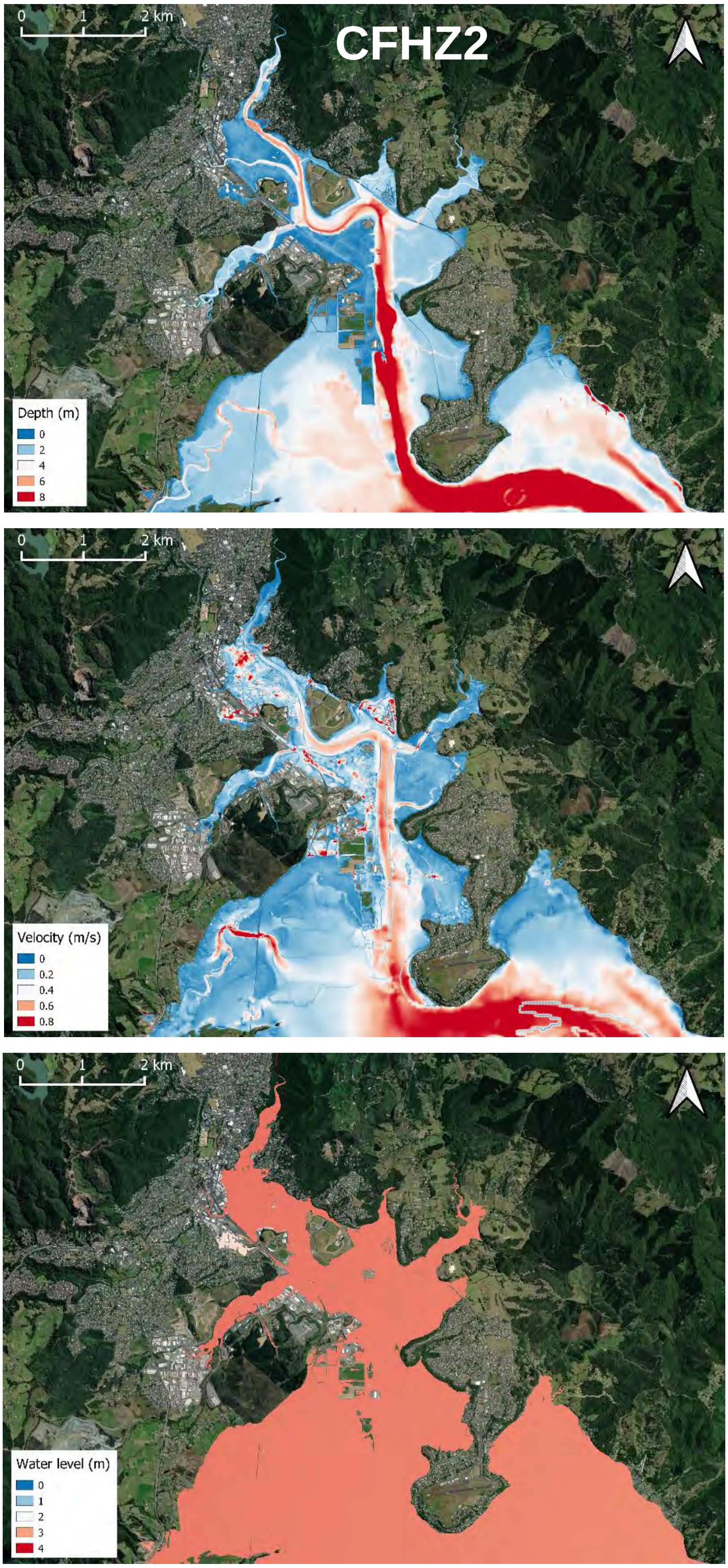

Figure A.3: Modelled maximum depth (upper), velocity (middle) and water level (lower) for the CFHZ2 scenario.

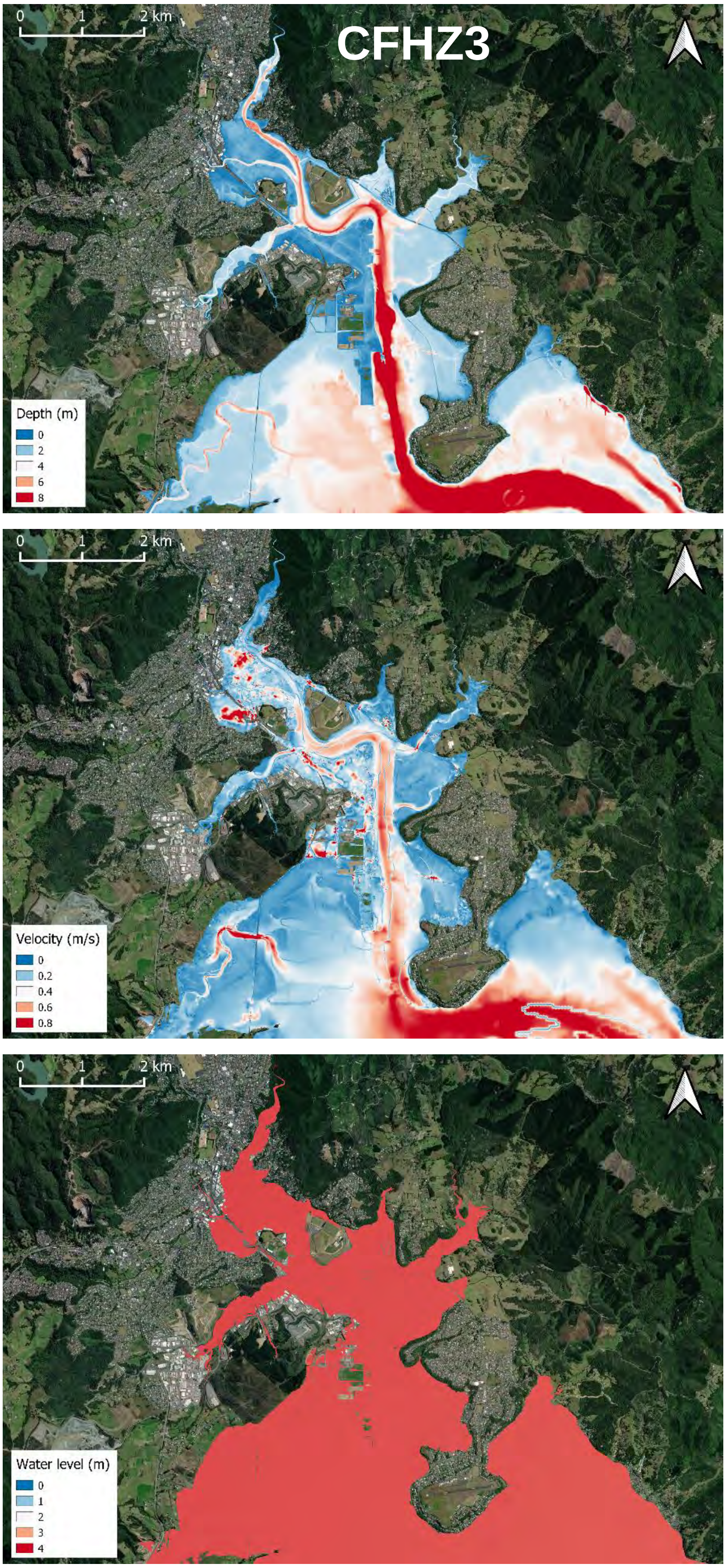

Figure A.4: Modelled maximum depth (upper), velocity (middle) and water level (lower) for the CFHZ3 scenario.

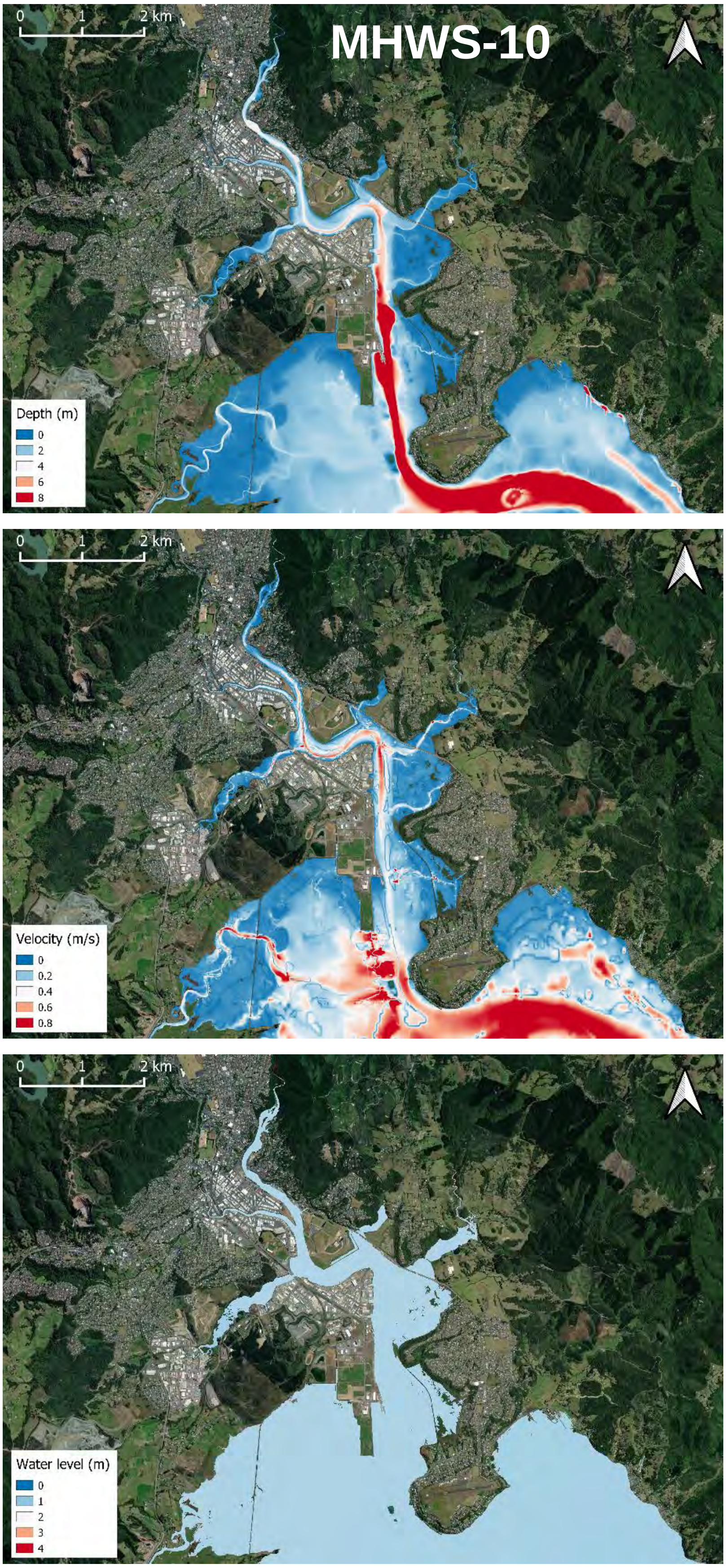

Figure A.5: Modelled maximum depth (upper), velocity (middle) and water level (lower) for the MHWS-10 scenario.

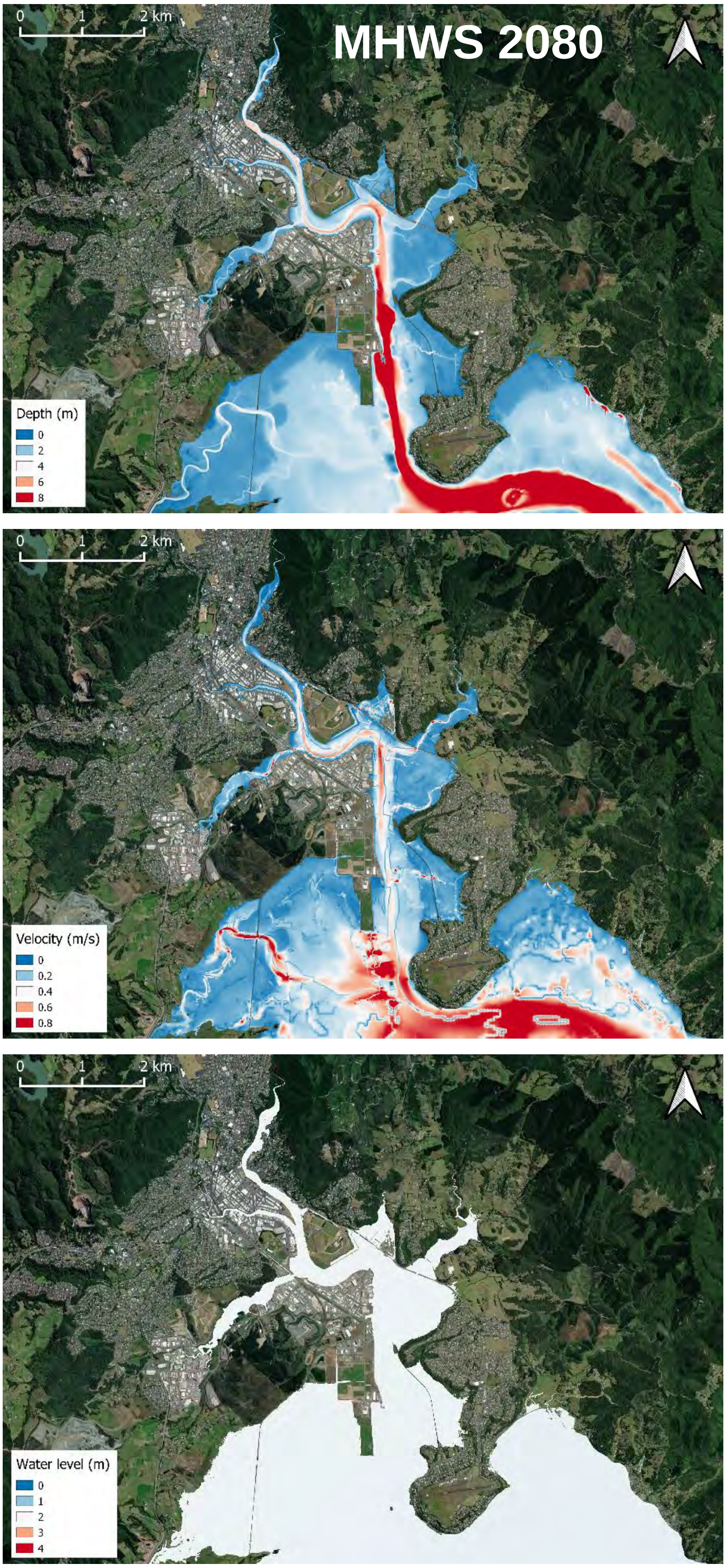

Figure A.6: Modelled maximum depth (upper), velocity (middle) and water level (lower) for the MHWS 2080 scenario.

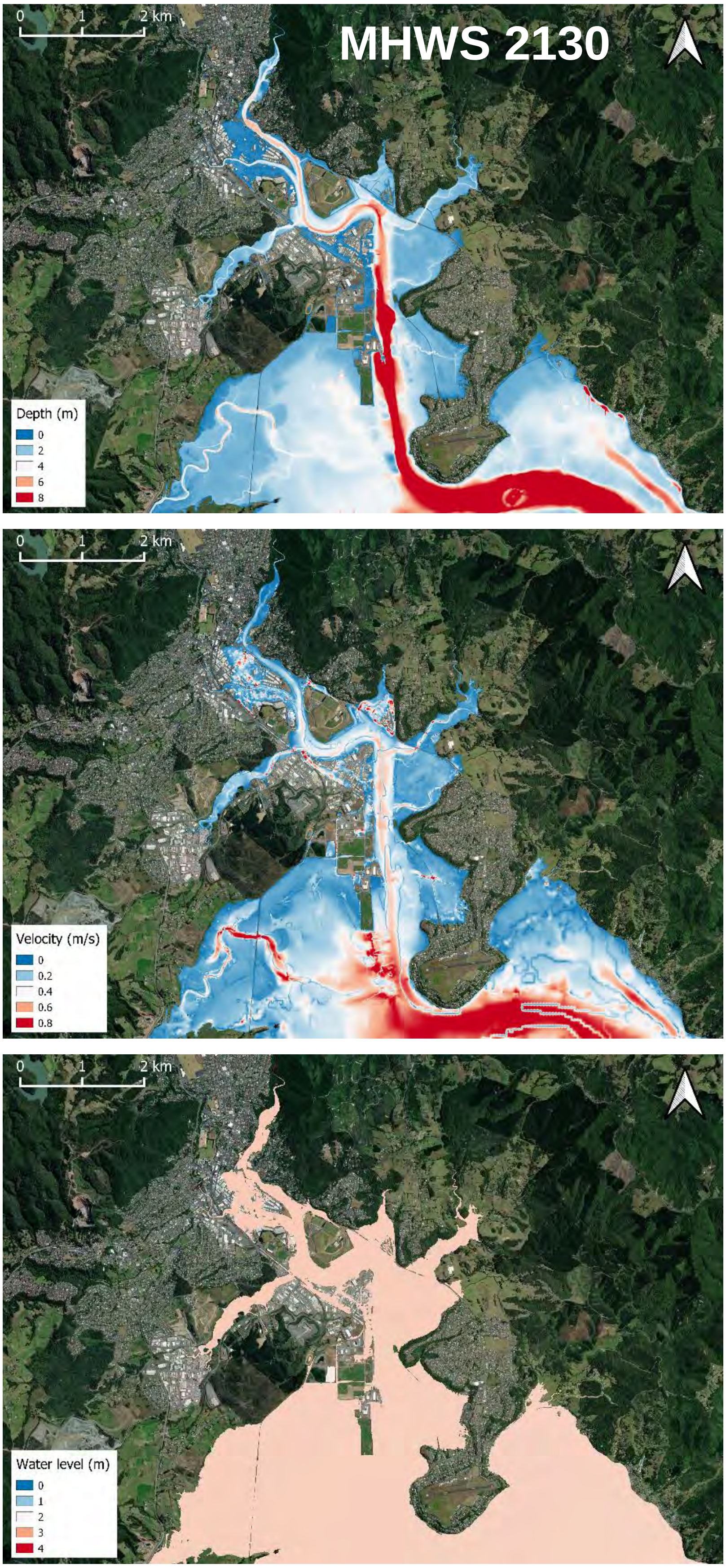

Figure A.7: Modelled maximum depth (upper), velocity (middle) and water level (lower) for the MHWS 2130 scenario.

Appendix B. Model Boundary Conditions

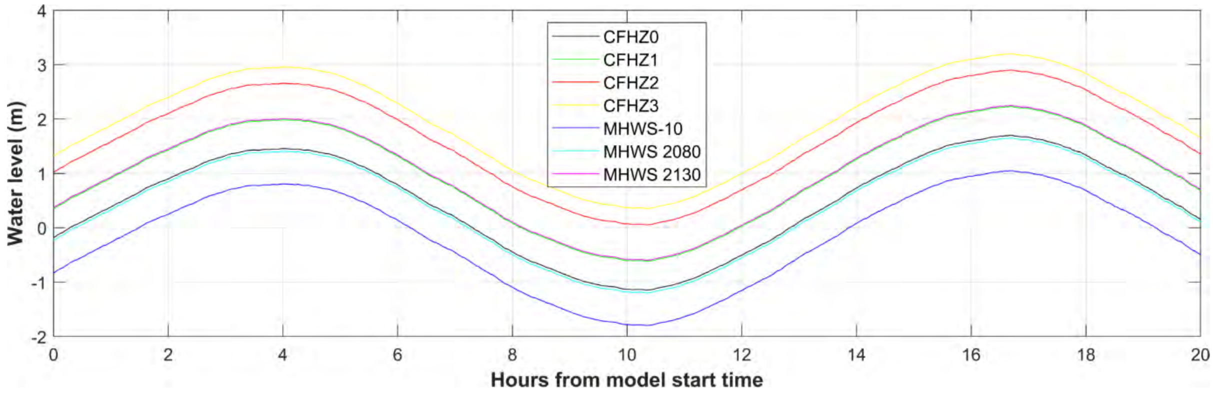

Figure B.1: Ocean boundary condition for Coastal Flood Hazard Zone (CFHZ) and Mean High Water Spring (MHWS) model runs. The peak of the second high tide matches the maximum water level values in Table 2.1. Note that CFHZ0 and MHWS 2080, as well as CFHZ1 and MHWS 2130, have similar maximum water levels, so are difficult to distinguish from one another in the figure.